



Original paper

Seismic Analysis of Unreinforced Masonry Walls

Jaya Prakash Vemuri¹, Subramaniam, Kolluru²

Received: 15/12/2015 / Accepted: 08/02/2017 / Published online: 11/03/2017

Abstract The Alpine-Himalayan belt which covers the entire Himalayan range of India is the second most active seismic belt in the world. In the Himalayan range, the Indian plate is in an on-going collision with the Eurasian plate. The consequent interlocking between the two plates causes a release of accumulated strain at several faults in this collision zone and leads to frequent inter-plate earthquakes. This region has a potential for high seismic activity in the future as well. Unreinforced, non-engineered brick masonry structures comprise a large percentage of buildings in the Himalayan region. Recent earthquakes have exposed the seismic vulnerability of such structures, which have been either severely damaged or have completely collapsed. Due to the high seismic hazard of the region and the inherent vulnerability of non-engineered masonry structures, a seismic assessment of masonry construction in this region is imperative.

A suite of strong ground motions is developed using data obtained from major Himalayan earthquakes. The response spectra and frequency plots for ground motions are examined. Ground motions are categorized using parameters such as peak ground acceleration, mean frequency, predominant frequency, Arias Intensity etc. Under seismic excitation, masonry exhibits significant displacement into the plastic range. Its hysteric behaviour is characterized by strength and stiffness degradation. In this study, Nonlinear Time History Analyses (NTHA) are performed on a Single Degree of Freedom (SDOF) model of an unreinforced masonry wall whose behaviour is simulated using the Modified-Takeda model. It is observed that the storey drifts exceed the prescribed drift limits under some severe ground motions. Further, the effect of various ground motion parameters on the structural response of masonry walls is examined. The Peak Ground Acceleration (PGA) is observed to be the most important parameter influencing the storey drift. No clear correlation was observed between storey drift and frequency content.

Key words Unreinforced masonry; Seismic assessment; Nonlinear time history analyses; Drift Peak ground acceleration; Himalayan region

1. INTRODUCTION

The Alpine-Himalayan region which covers the entire Himalayan range of India is the second most active seismic belt in the world (Sinvhal 2010) and has a potential for high seismic activity in the future

¹ Ph.D. Student, Department of Civil Engineering, IIT Hyderabad, ce13p1006@iith.ac.in

² Professor, Department of Civil Engineering, IIT Hyderabad, kvls@iith.ac.in

as well. A large percentage of the building stock in the Himalayan region consists of non-engineered, unreinforced brick masonry (URM) structures, unreinforced adobe or block masonry structures. The percentage of building stock that is composed of unreinforced adobe, block masonry, and brick masonry construction in India obtained from Prompt Assessment of Global Earthquakes for Response (PAGER) survey is 69% for Unreinforced Fired Brick masonry (WHE-PAGER Survey 2007). Typically, such structures consist of load-bearing masonry walls, made of low strength bricks. Recent Himalayan earthquakes have exposed the seismic vulnerability of such structures, which have been either severely damaged or have completely collapsed (Shrikhande et al. 2000). Traditional clay brick masonry structures performed poorly and shear failure of brick walls was noticed with diagonal cracks. Due to the high seismic hazard of the Himalayan region and the inherent vulnerability of non-engineered low strength masonry structures, which comprise the bulk of structures in this region, a seismic assessment of masonry construction is imperative.

Assessment of the seismic vulnerability of URM buildings requires a methodology for assessing the performance of such structures subjected to horizontal forces generated by earthquake ground motion. However, most of the available literature on masonry is focused on out of plane masonry behaviour or on reinforced masonry walls. Failure of URM walls, which has been predominantly observed in the Himalayan rural dwellings (Shrikhande *et al.* 2000) is an area that has not been well investigated. Only limited experimental studies are available on the behaviour of unreinforced clay brick walls (Magenes and Calvi 1997; Abrams 1992). Other research on in-plane wall behaviour is inconsistent and vary widely. Most of the research does not provide simple predictive equations for strength and stiffness (FEMA 1999).

In the past, lack of seismographs in the Himalayan region, combined with the absence of data sharing mechanism across government organizations, has contributed to a poor understanding of the actual uncertainty due to ground motion in the Himalayas. The absence of standardized construction practices contributes to uncertainty in building quality. Hence, due to the high seismic hazard of the Himalayan region and the inherent vulnerability of non-engineered low strength masonry structures, which comprise the bulk of structures in this region, a seismic assessment of masonry construction is imperative. Further, as uncertainty in ground motion strongly depends on the local site conditions and geological profile of the area, for an accurate seismic assessment of URM walls, it is important to characterize the local ground motions recorded in the Himalayas. The effect of ground motion parameters, such as PGA, frequency content and Arias intensity on observed damage to URM walls, have not been accounted in literature. No detailed correlation study between seismic parameters and damage indices for URM walls is available. A study by Elenas and Meskouris (2001) reports the correlation between seismic parameters and damage in multistorey concrete buildings. A similar study for URM walls is imperative to understand variation in structural response.

In this study, a suite of strong ground motions is developed using data acquired from Consortium of Organisations for Strong-Motion Observation Systems (COSMOS) for two major Himalayan earthquakes: the 1991 Uttarkashi earthquake and the 1999 Chamoli earthquake. The response spectra of these ground motions, as seen in Figure 1, exhibit 'peaks' in the low period range, thus indicating the concentration of high energy in the short period range.

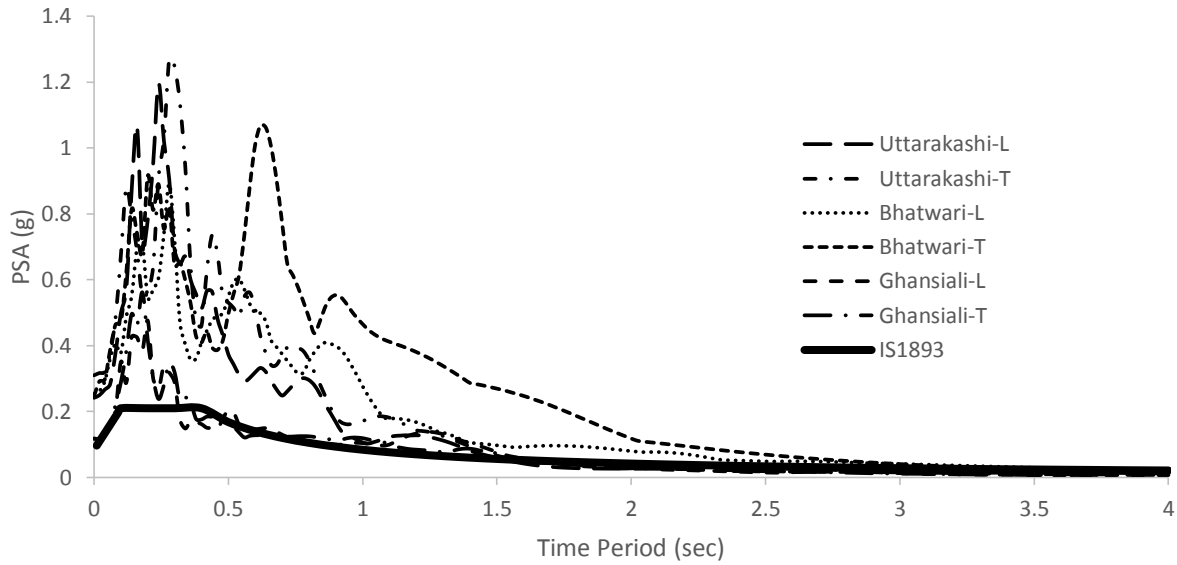


Figure 1. Response Spectra of Ground Motions (1991 Uttarkashi Earthquake)

2. HYSTERIC MODEL

Nonlinear Time History Analyses (NTHA) are performed on a Single Degree of Freedom (SDOF) unreinforced masonry (URM) wall. Figure 2a shows the SDOF model of a masonry wall. The Unreinforced Masonry (URM) Wall has a height of 1000 mm, a length of 4240 mm, a thickness of 240 mm thick and a total mass of 10000 kg (Vera and Chow 2008). The compressive strength of soft mortar and stiff bricks are 1 and 12 MPa, respectively. The Young's Modulus is 7000 MPa and 12000 MPa, respectively. The damping ratio, ζ is 15% and the natural frequency is 2 Hz.

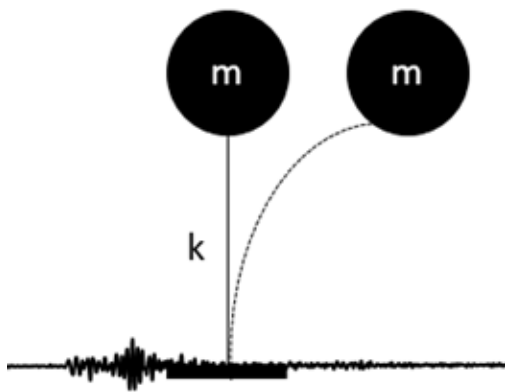


Figure 2. (a) SDOF Model of the URM Wall

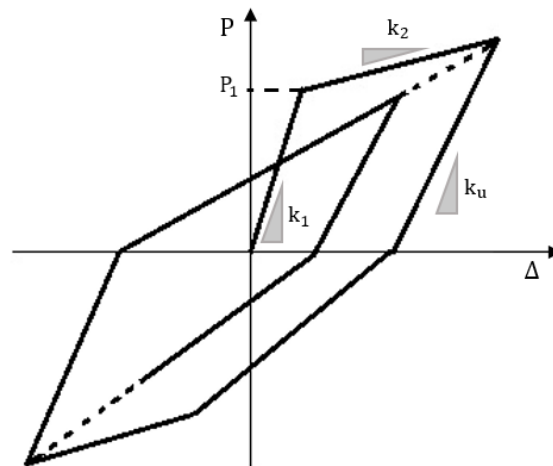


Figure 2. (b) The Modified Takeda Model

Under seismic excitation, masonry exhibits significant displacement into the plastic range. Its hysteric behaviour is characterized by strength and stiffness degradation. This behaviour is simulated using the

Modified-Takeda model, seen in Figure 2b. The model has been used by researchers to study URM walls (Lumanterna *et al.* 2006, Vaculik *et al.* 2007). The model used in the present study is calibrated by Vera and Chouw (2008) and is used with the characteristic values as follows:

$$SR = \frac{P_1}{mg} = 0.232, \alpha = \frac{k_2}{k_1} = 0.168, k_u = k_1 \left(\frac{d_y}{d_{max}} \right)^q \text{ with } q = 0.4$$

Here, α is the ratio of post-elastic stiffness, k_2 to the elastic stiffness, k_1 . SR is the ratio of the yield force to the structural weight, k_u is the return slope, d_y is the yield displacement and d_{max} is the maximum displacement.

3. RESULTS FROM NONLINEAR TIME HISTORY ANALYSES

The hysteric behaviour of the masonry wall under NTHA is compared with that of qualitative graphs available from the literature. The Modified –Takeda model is observed to represent the strength and stiffness degradation well. To minimize damage to structures, the ASCE/SEI-7-05 prescribes limits for storey drift. These limits are specified in Table 1. As the height of the masonry wall is 1000mm, the maximum allowable drift (1%) is 10mm. It is observed that under severe ground motions, the masonry wall exhibits drifts that exceed the code prescribed limits, thus indicating severe damage and/or collapse.

Table 1. Allowable Storey Drifts, Δ_a as per ASCE/SEI-7-05 (Note: h_{sx} is the storey height)

| S.No. | Structure | Occupancy Category | | |
|-------|--|--------------------|----------------|----------------|
| | | I or II | III | IV |
| 1 | Structures, other than masonry shear wall structures, four stories or less with interior walls, partitions, ceilings, and exterior wall systems that have been designed to accommodate the storey drifts | 0.025 h_{sx} | 0.020 h_{sx} | 0.015 h_{sx} |
| 2 | Masonry Cantilever Shear Wall Structures | 0.010 h_{sx} | 0.010 h_{sx} | 0.010 h_{sx} |
| 3 | Other masonry shear wall structures | 0.007 h_{sx} | 0.007 h_{sx} | 0.007 h_{sx} |
| 4 | All other structures | 0.020 h_{sx} | 0.015 h_{sx} | 0.010 h_{sx} |

Results from the NTHA on the masonry wall are shown in Tables 2 and 3. The results indicate that the maximum and average value of drifts, computed using records of the Uttarkashi earthquake, were 40.69 mm and 6.99 mm, respectively. The standard deviation of the drift is 8.59mm. Similarly, the maximum and average value of drifts, computed using records of the Chamoli earthquake, was observed to be 55.54 mm and 6.67 mm, respectively. The standard deviation of the drift is 11.56mm. It is observed that the average values of drift obtained from the suite of accelerograms from the Uttarkashi and Chamoli earthquakes are quite close. Clearly, under some severe ground motions of the 1991 Uttarkashi earthquake and the 1999 Chamoli Earthquake, the masonry wall under investigation is observed to exceed these prescribed drift limits.

Two ground motion parameters, Peak Ground Acceleration (PGA) and Arias Intensity (AI) are correlated with two structural response parameters, drift and floor acceleration.

- a) **Storey Drift:** As seen in Figure 3, most ground motions of the 1991 Uttarkashi earthquake have low PGA values (<0.1g) and the observed drift is observed to be lower than the code prescribed limit of 10mm. However, four ground motions, namely *Bhatwari-L*, *Bhatwari-T*, *Uttarakashi-L*,

and *Uttarakashi-T*, having high PGA are observed to cause drifts which exceed code prescribed limits.

As seen in Figure 4, a similar trend is observed in the 1999 Chamoli earthquake. Two ground motions, namely *Gopeshwar-L* and *Gopeshwar-T*, with high PGA values, are observed to cause drifts which exceed code prescribed limits.

- b) **Floor Acceleration:** The floor acceleration in the present case is the acceleration of the top of the wall. The floor accelerations have a linearly increasing trend with the PGA, as shown in Figure 5. No code provisions exist for correlating Floor Acceleration (FA) to damage. The same four ground motions, namely *Bhatwari-L*, *Bhatwari-T*, *Uttarkashi-L*, and *Uttarkashi-T*, having high PGA are observed to result in high floor acceleration values.

A similar trend is observed in Figure 6, for results from the Chamoli earthquake: the floor acceleration shows a strong correlation with PGA. Two ground motions, namely *Gopeshwar-L* and *Gopeshwar-T* having high PGA are observed to cause high floor accelerations.

The Arias Intensity represents the energy content of the seismic wave (Arias 1970). The overall energy content of a seismic wave may contribute to energy absorption by the structure and consequently cause damage. Figures 7 and 8 indicate that for the 1991 Uttarakashi quake, storey drift and floor acceleration and exhibit a strong correlation with Arias Intensity. Similarly, for the 1999 Chamoli earthquake, both drift and floor acceleration show a strong correlation with Arias Intensity, as seen in Figures 9 and 10.

The URM wall exhibits markedly different peak responses (storey drift and floor acceleration) in high PGA ground motions. These ground motions having similar values of high PGA were recorded at stations situated at varying distances from the epicenter. In such cases, the frequency of the strong ground motion was observed to influence the drift. As an example, the record *Bhatwari-T* with a PGA of 0.253g is observed to have a predominant period of 0.62seconds, which is close to the natural period of the structure and is observed to result in a high value of drift of 40.69mm. The *Bhatwari-L* record with a PGA of 0.247g, has a much lower predominant period of 0.28 seconds results in a drift of 20.01 mm.

The ground motion frequency content is represented well using single parameters, such as Mean Period, T_p and Predominant Period, T_m , which are also tabulated in Tables 2 and 3.

Table 2. 1991 Uttarkashi Earthquake: Summary of Results

| S.No | EQ record | Soil Type | Dist. | PGA (g) | Frequency | | Arias Intensity (m/s) | Drift (mm) | Floor Acc. |
|------|---------------|-----------|-------|---------|-------------|-------------|-----------------------|------------|------------|
| | | | (km) | | T_p (sec) | T_m (sec) | | U_{max} | FA (g) |
| 1 | Almora-L | A | 158 | 0.018 | 0.26 | 0.39 | 0.007 | 1.38 | 0.0268 |
| 2 | Almora-T | A | 158 | 0.021 | 0.22 | 0.40 | 0.007 | 1.47 | 0.0297 |
| 3 | Barkot-L | A | 53 | 0.082 | 0.12 | 0.23 | 0.134 | 6.47 | 0.159 |
| 4 | Barkot-T | A | 53 | 0.095 | 0.26 | 0.25 | 0.108 | 4.71 | 0.116 |
| 5 | Bhatwari-L | A | 53 | 0.247 | 0.28 | 0.42 | 0.726 | 20.01 | 0.331 |
| 6 | Bhatwari-T | A | 53 | 0.253 | 0.62 | 0.54 | 1.114 | 40.69 | 0.375 |
| 7 | Ghansiali-L | A | 42 | 0.117 | 0.2 | 0.30 | 0.238 | 7.39 | 0.226 |
| 8 | Ghansiali-T | A | 42 | 0.118 | 0.18 | 0.26 | 0.301 | 7.06 | 0.179 |
| 9 | Karnprayag-L | A | 73 | 0.062 | 0.34 | 0.34 | 0.075 | 3.66 | 0.091 |
| 10 | Karnprayag-T | A | 73 | 0.079 | 0.34 | 0.33 | 0.064 | 4.59 | 0.125 |
| 11 | Kosani-L | A | 152 | 0.029 | 0.2 | 0.25 | 0.011 | 0.99 | 0.035 |
| 12 | Kosani-T | A | 152 | 0.032 | 0.18 | 0.24 | 0.013 | 1.48 | 0.036 |
| 13 | Koteshwar-L | A | 64 | 0.101 | 0.24 | 0.30 | 0.211 | 5.76 | 0.143 |
| 14 | Koteshwar-T | A | 64 | 0.067 | 0.28 | 0.33 | 0.078 | 3.64 | 0.096 |
| 15 | Koti-L | A | 98 | 0.042 | 0.34 | 0.54 | 0.006 | 1.93 | 0.032 |
| 16 | Koti-T | A | 98 | 0.021 | 0.36 | 0.45 | 0.016 | 3.79 | 0.078 |
| 17 | Purola-L | A | 67 | 0.075 | 0.2 | 0.29 | 0.052 | 4.67 | 0.117 |
| 18 | Purola-T | A | 67 | 0.094 | 0.18 | 0.29 | 0.097 | 3.75 | 0.127 |
| 19 | Rudraprayag-L | A | 60 | 0.053 | 0.12 | 0.15 | 0.110 | 2.40 | 0.063 |
| 20 | Rudraprayag-T | A | 60 | 0.052 | 0.12 | 0.17 | 0.091 | 3.32 | 0.075 |
| 21 | Srinagar-L | A | 62 | 0.067 | 0.08 | 0.16 | 0.084 | 1.78 | 0.074 |
| 22 | Srinagar-T | A | 62 | 0.050 | 0.08 | 0.19 | 0.055 | 1.99 | 0.05 |
| 23 | Tehri-L | A | 53 | 0.073 | 0.32 | 0.42 | 0.058 | 4.26 | 0.09 |
| 24 | Tehri-T | A | 53 | 0.062 | 0.26 | 0.71 | 0.068 | 4.78 | 0.076 |
| 25 | Uttarakashi-L | A | 31 | 0.242 | 0.24 | 0.29 | 0.756 | 14.95 | 0.392 |
| 26 | Uttarakashi-T | A | 31 | 0.310 | 0.30 | 0.34 | 0.963 | 24.75 | 0.527 |

Table 3. 1999 Chamoli Earthquake: Summary of Results

| S.No | EQ record | Soil Type | Dist. | PGA (g) | Frequency | | Arias Intensity (m/s) | Drift (mm) | Floor Acc. |
|------|----------------|-----------|-------|---------|-------------|-------------|-----------------------|------------|------------|
| | | | (km) | | T_p (sec) | T_m (sec) | | U_{max} | FA (g) |
| 1 | Almora-L | A | 106 | 0.027 | 0.24 | 0.35 | 0.011 | 1.90 | 0.038 |
| 2 | Almora-T | A | 106 | 0.028 | 0.26 | 0.36 | 0.008 | 2.49 | 0.039 |
| 3 | Barkot-L | A | 118 | 0.023 | 0.18 | 0.26 | 0.002 | 0.68 | 0.019 |
| 4 | Barkot-T | A | 118 | 0.017 | 0.22 | 0.25 | 0.005 | 0.98 | 0.029 |
| 5 | Chinaylisaur-L | A | 103 | 0.045 | 0.32 | 0.37 | 0.036 | 4.09 | 0.098 |
| 6 | Chinaylisaur-T | A | 103 | 0.052 | 0.3 | 0.40 | 0.047 | 5.58 | 0.092 |
| 7 | Ghansiali-L | A | 73 | 0.083 | 0.18 | 0.24 | 0.110 | 3.12 | 0.09 |
| 8 | Ghansiali-T | A | 73 | 0.073 | 0.18 | 0.24 | 0.142 | 3.23 | 0.111 |
| 9 | Gopeshwar-L | A | 14 | 0.197 | 0.66 | 0.79 | 0.290 | 19.25 | 0.248 |
| 10 | Gopeshwar-T | A | 14 | 0.356 | 0.36 | 0.67 | 0.799 | 55.54 | 0.48 |
| 11 | Joshimath-L | A | 17 | 0.064 | 0.16 | 0.41 | 0.033 | 3.08 | 0.093 |
| 12 | Joshimath-T | A | 17 | 0.071 | 0.24 | 0.78 | 0.058 | 4.57 | 0.094 |
| 13 | Lansdowne-L | A | 102 | 0.005 | 0.16 | 0.25 | 0.000 | 0.30 | 0.0057 |
| 14 | Lansdowne-T | A | 102 | 0.006 | 0.1 | 0.20 | 0.000 | 0.23 | 0.008 |
| 15 | Roorkee-L | C | 162 | 0.047 | 1.46 | 1.78 | 0.176 | 4.64 | 0.0222 |
| 16 | Roorkee-T | C | 162 | 0.056 | 1.32 | 1.83 | 0.131 | 3.68 | 0.0219 |
| 17 | Tehri-L | A | 88 | 0.054 | 0.3 | 0.42 | 0.044 | 6.84 | 0.123 |
| 18 | Tehri-T | A | 88 | 0.062 | 0.44 | 0.47 | 0.042 | 6.25 | 0.111 |
| 19 | Ukhimath-L | A | 29 | 0.097 | 0.28 | 0.42 | 0.081 | 5.73 | 0.131 |
| 20 | Ukhimath-T | A | 29 | 0.091 | 0.28 | 0.37 | 0.082 | 5.01 | 0.123 |
| 21 | Uttarakashi-L | A | 94 | 0.064 | 0.2 | 0.37 | 0.031 | 3.91 | 0.074 |
| 22 | Uttarakashi-T | A | 94 | 0.053 | 0.4 | 0.33 | 0.049 | 4.52 | 0.124 |

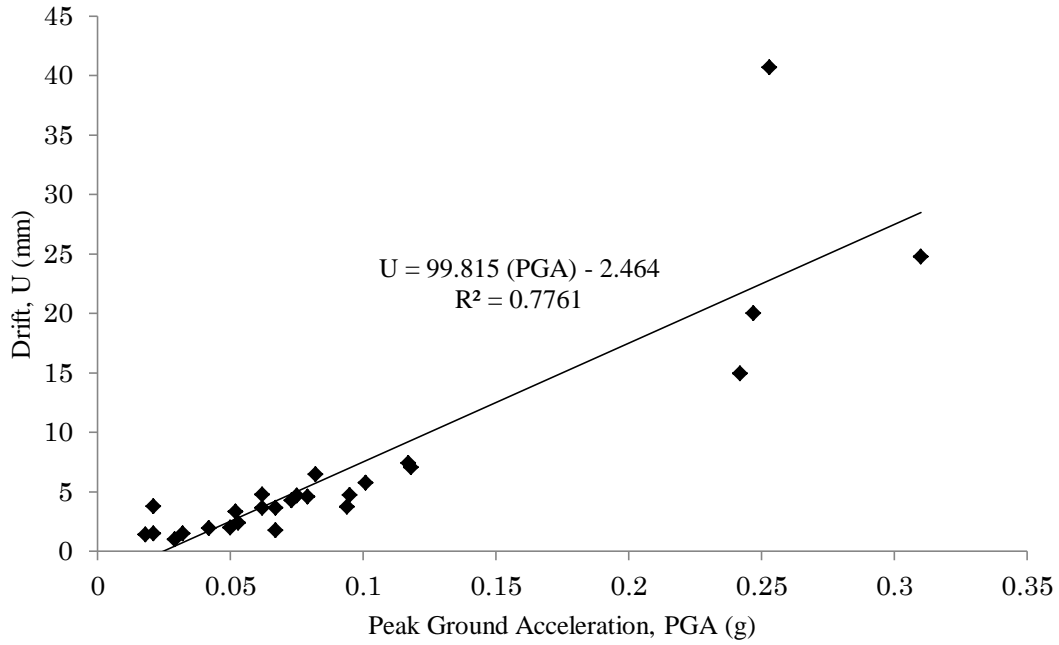


Figure 3. Drift versus Peak Ground Acceleration (1991 Uttarkashi Earthquake)

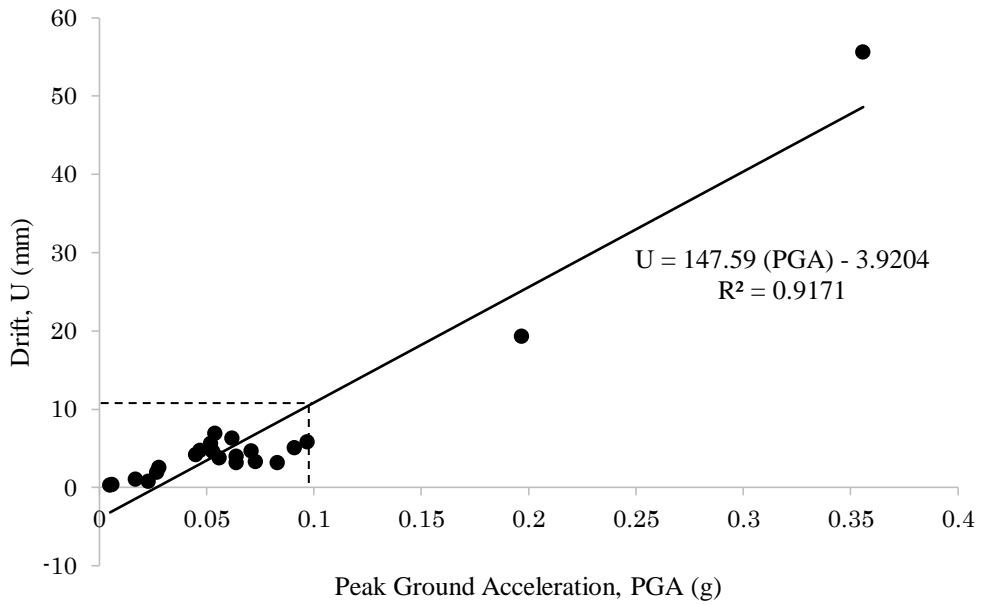


Figure 4. Drift versus Peak Ground Acceleration (1999 Chamoli Earthquake)

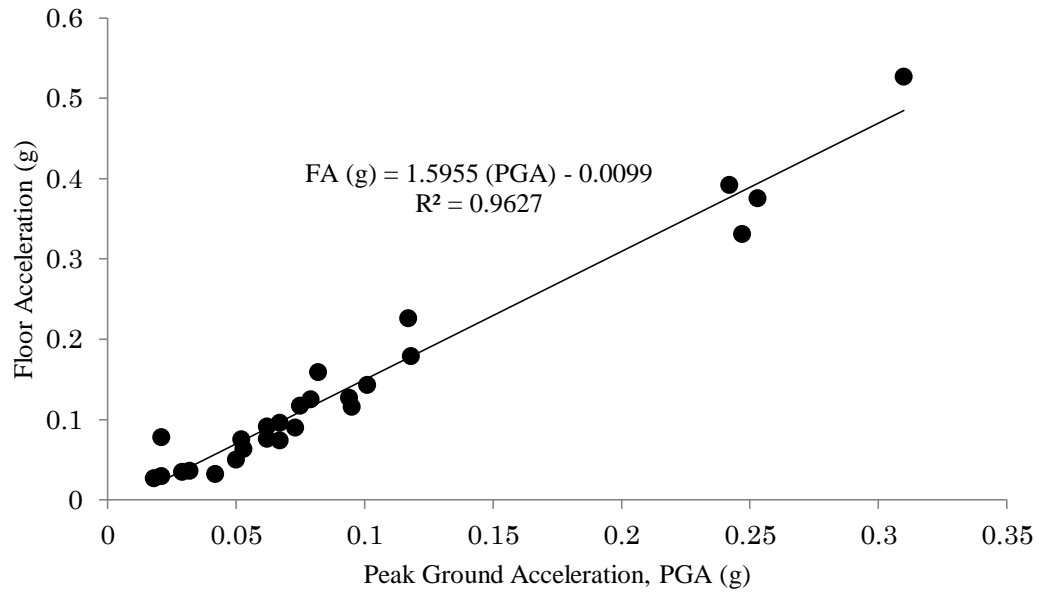


Figure 5. Floor Acceleration versus Peak Ground Acceleration (1991 Uttarakashi Quake)

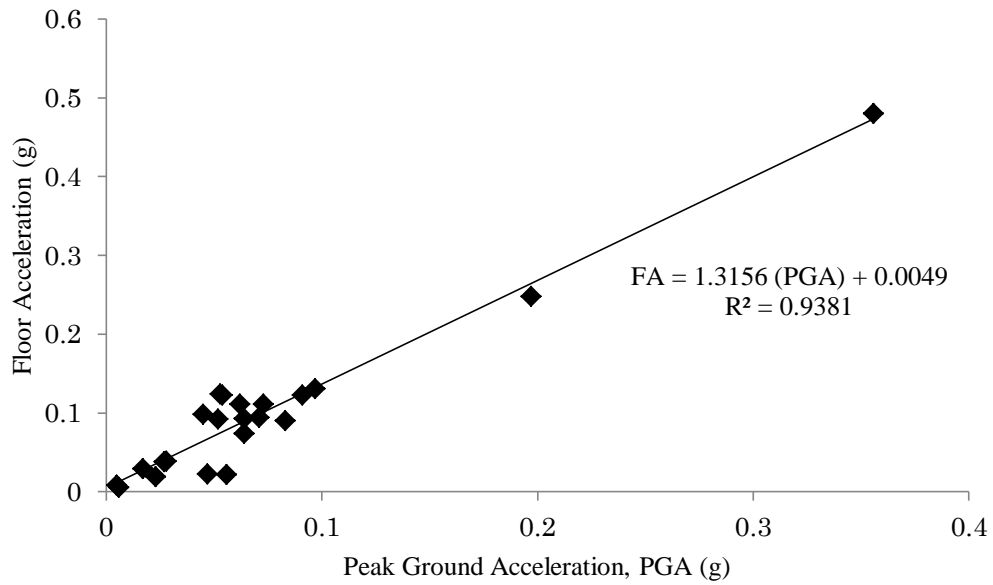


Figure 6. Floor Acceleration versus Peak Ground Acceleration (1999 Chamoli Earthquake)

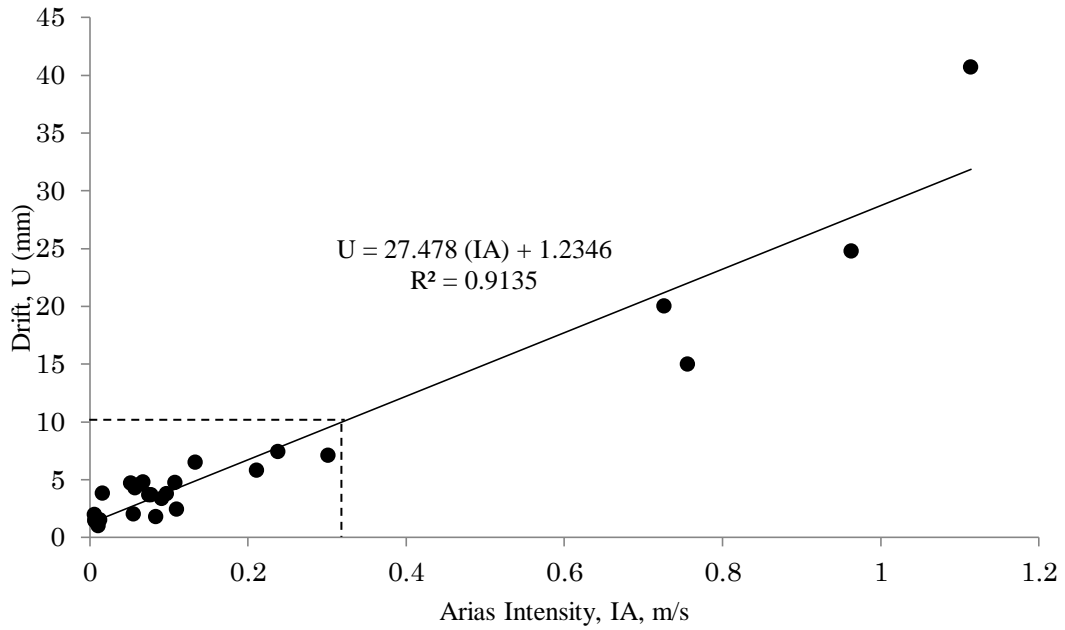


Figure 7. Drift versus Arias Intensity (1991 Uttarkashi Earthquake)

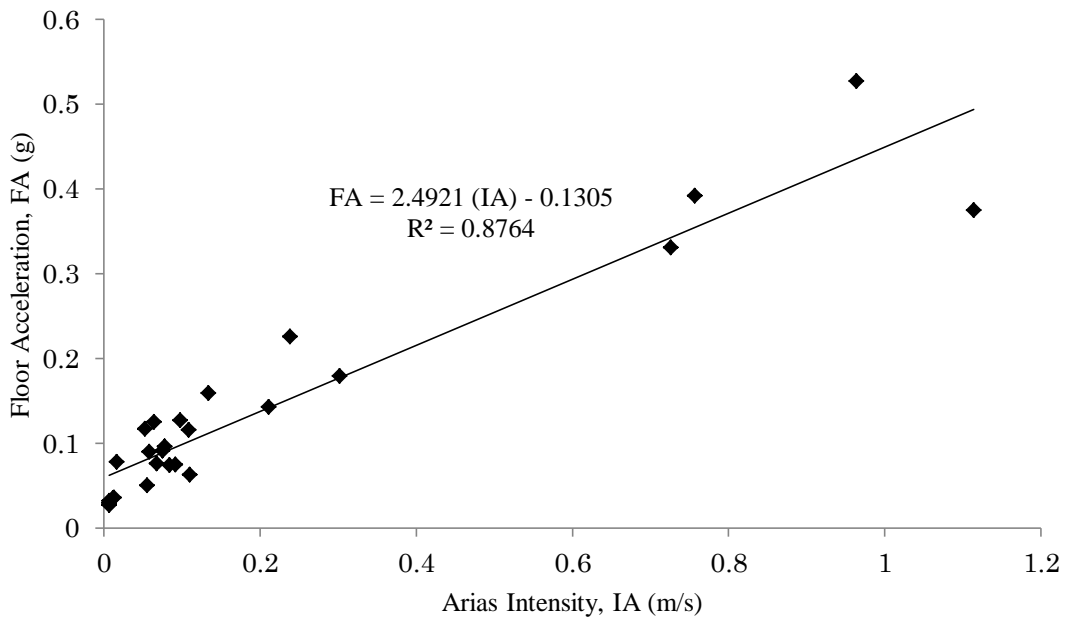


Figure 8. Floor Acceleration versus Arias Intensity (1991 Uttarkashi Earthquake)

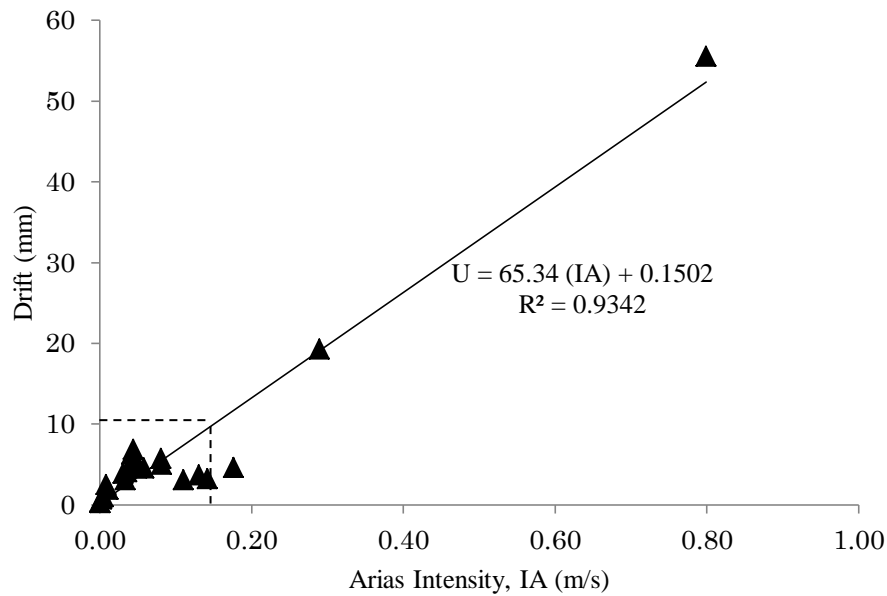


Figure 9. Drift versus Arias Intensity (1999 Chamoli Earthquake)

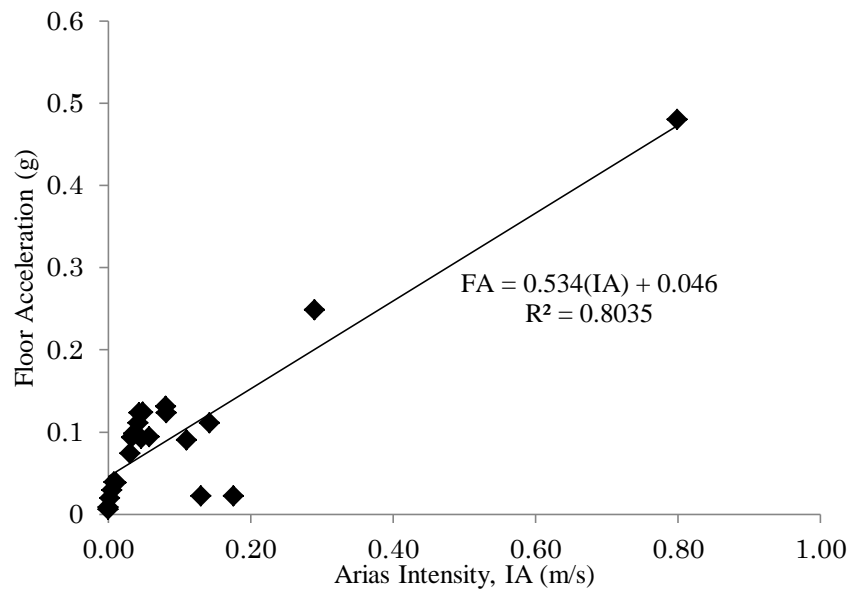


Figure 10. Floor Acceleration versus Arias Intensity (1999 Chamoli Earthquake)

4. EFFECT OF GROUND MOTION FREQUENCY

The predominant period, T_p is defined as the period at which the maximum spectral acceleration occurs in a 5% damped acceleration response spectrum. It can also be obtained as the period of vibration corresponding to the maximum value of the Fourier Amplitude Spectrum. T_p can only indicate the location of the peak in the acceleration response spectrum but cannot describe the dispersion of the

frequency content around the peak (Rathje 1998). The mean period, T_m represents the average frequency content and is estimated by equation [1] where C_i are the Fourier amplitudes, and f_i represents the discrete Fourier transform frequencies between 0.25 and 20 Hz. T_m is similar to the mean square frequency, which is estimated using equation [1] with the term $1/f_i$ replaced by f_i . In Tables 2 and 3, the predominant and mean period of each wave was also tabulated.

$$T_m = \frac{\sum (C_i^2)}{\sum C_i^2 f_i} \quad [1]$$

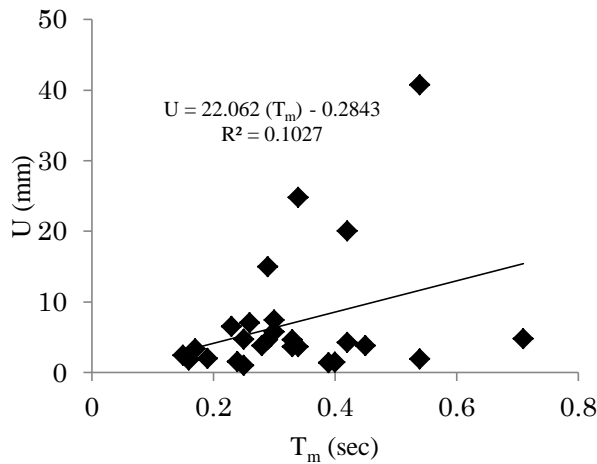


Figure 11. (a) Drift vs Mean Period (Uttarakashi)

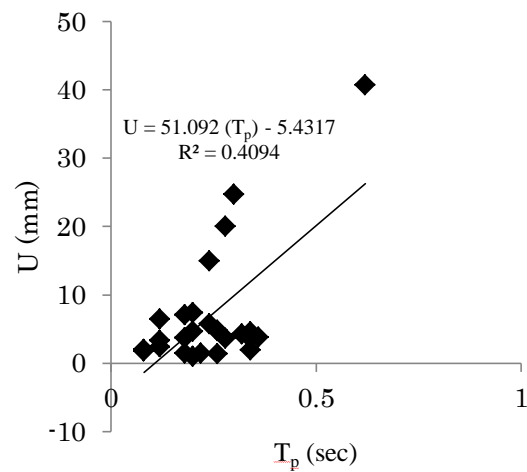


Figure 11. (b) Drift vs Predominant Period (Uttarakashi)

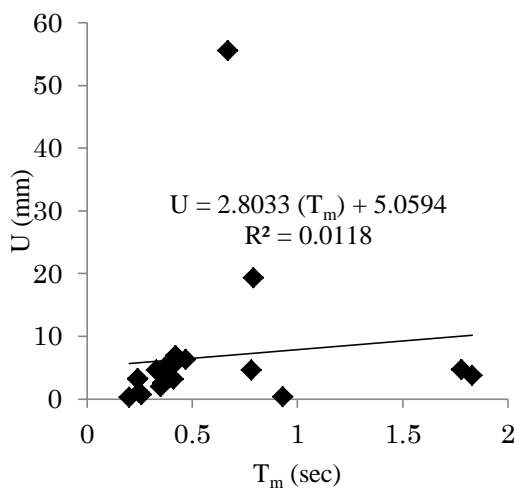


Figure 12. (a) Drift vs Mean Period (Chamoli)

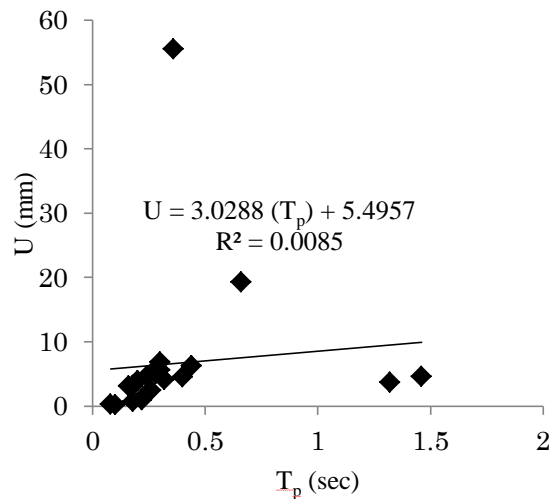


Figure 12. (b) Drift vs Predominant Period (Chamoli)

Figures 11 and 12 show the weak correlation between the drift and the mean period and predominant

period, respectively for the 1991 Uttarkashi Earthquake and the 1999 Chamoli earthquake. The weak correlation indicates that the frequency content of the earthquake is a secondary parameter which may explain damage in only certain cases.

5. SUMMARY AND CONCLUSIONS

In this study, seismic assessment of unreinforced masonry walls is performed using nonlinear time history analyses. Ground motions from two major Himalayan earthquakes were considered. The following major conclusions may be drawn from this study –

- a) The response spectra of the ground motions show ‘peaks’ in the low period range and exceed the code prescribed spectra. This indicates that low-rise structures with low natural time periods are especially susceptible to damage.
- b) The data from the nonlinear time history analyses indicate that the characteristics of the ground motion vary significantly among recording stations. There are three main causes for observed variation in ground motion parameters: the source, the travelled path, and the site conditions. The effect of these manifests in the form of varied amplitude and varied frequency content of the recorded wave. This study highlights the frequency content of the 1991 Uttarakashi and 1999 Chamoli earthquakes using simple single frequency parameters, i.e. mean period and predominant period.
- c) The Modified Takeda model is used to simulate the behaviour of the masonry wall and is observed to represent the strength and stiffness degradation well. It is observed that the storey drifts exceed the code prescribed drift limits under severe ground motions.
- d) The effect of the amplitude and frequency characteristics on the observed structural response has been discussed in detail in this study. The Peak Ground Acceleration (PGA) exhibits a linearly increasing relationship with the observed drift and is observed to be the most important parameter influencing the Storey Drift.
- e) A key finding of this study was to observe the effect of frequency on the structural response. Ground motions having similar values of high PGA were recorded at different stations situated at varying distances from the epicenter. However, under these ground motions with similar high PGA, the unreinforced masonry wall exhibits markedly different peak responses, i.e. a high variation in storey drift and floor accelerations is observed. In such cases, the frequency of the strong ground motion was observed to cause resonance and influence the drift.
- f) The Floor Acceleration is also observed to have a linearly increasing relationship with the PGA. However, no codal provisions are available to define floor acceleration limits with damage.
- g) The Arias Intensity represents the energy content in the seismic wave. The storey drift and Floor Acceleration are also observed to exhibit a strong correlation with the Arias Intensity.

The findings of this study may be further generalized by considering different types of unreinforced masonry walls prevalent in the Himalayan region.

REFERENCES

- Abrams, D.P. (1992), Strength and Behavior of Unreinforced Masonry Elements, *Proceedings of the Tenth World Conference on Earthquake Engineering*, Balkema, Rotterdam, pp.3475-3480
- American Society of Civil Engineers. (2006) *Minimum Design Loads for Buildings and Other Structures*, ASCE/SEI-7-05, Reston, VA
- Arias, A. (1970) A measure of earthquake intensity, in R.J. Hansen, ed. *Seismic Design for Nuclear Power Plants*, MIT Press, Cambridge, Massachusetts, 438-483
- Consortium of Organizations for Strong-Motion Observation Systems (COSMOS), www.cosmos-eq.org (last accessed in July 2015)
- Elenas, A. and Meskouris, K. (2001) Correlation study between seismic acceleration parameters and damage indices of structures, *Engineering Structures*, Vol. 23, pp. 698-704
- Federal Emergency Management Agency (1999) *Evaluation of Earthquake Damaged Concrete and Masonry Wall buildings: Technical Resources*, FEMA P-307, Washington D.C.
- Lumanterna, E., Vaculik, J., Griffith, M. Lam, N. and Wilson, J. (2006) Seismic Fragility Curves for Unreinforced Masonry Walls, *Proceedings of the Earthquake Engineering in Australia Conference*, Canberra
- Magenes, G. and Calvi, G.M., (1997) In-plane seismic response of brick masonry walls, *Earthquake Engineering and Structural Dynamics*, Vol. 26, pp. 1091-1112
- Rathje, E.M., Abrahamson, N.A., and Bray, J.D. (1998) Simplified Frequency Content Estimates of Earthquake Ground Motions, *Journal of Geotechnical and Geoenvironmental Engineering*, ASCE, 124(2), 150-159.
- Shrikhande, M., Rai, D.C., Narayan, J and Das, J. (2000) The March 29 Earthquake at Chamoli, India, *Proceedings of the 12th World Conference on Earthquake Engineering*, Auckland, New Zealand
- Sinvhal, A. (2010) *Understanding Earthquake Disasters*, Tata Mc-Graw Hill Education Private Limited, India, pp.320
- Vaculik, J., Lumanterna, E., Griffith, M. Lam, N. and Wilson, J. (2007): "Dynamic Fragility Curves for Unreinforced Masonry Walls", *Proceedings of the Australian Earthquake Engineering Society Conference*, Wollongong, NSW
- Vera, C.O. and Chouw, N. (2008) Comparison of record scaling methods proposed by standards currently applied in different countries, *Proceedings of the 14th World Conference on Earthquake Engineering*, Beijing, China
- WHE-PAGER Survey (2007): <http://www.world-housing.net/related-projects/whe-pager-project/about-this-project> (last accessed in July 2015)